Journal of Experimental Botany, Vol. 63, No. 5, pp. 1951–1967, 2012
doi:10.1093/jxb/err393 Advance Access publication 7 December, 2011
This paper is available online free of all access charges (see http://jxb.oxfordjournals.org/open_access.html for further details)

Journal of Experimental Botany
www.jxb.oxfordjournals.org

RESEARCH PAPER

Identification, functional characterization, and regulation of the enzyme responsible for floral (*E*)-nerolidol biosynthesis in kiwifruit (*Actinidia chinensis*)

Sol A. Green[1,*], Xiuyin Chen[1], Niels J. Nieuwenhuizen[1], Adam J. Matich[2], Mindy Y. Wang[1], Barry J. Bunn[2], Yar-Khing Yauk[1] and Ross G. Atkinson[1]

[1] The New Zealand Institute for Plant & Food Research Limited, Private Bag 92 169, Auckland, New Zealand
[2] The New Zealand Institute for Plant & Food Research Limited, Private Bag 11 600, Auckland, New Zealand

* To whom correspondence should be addressed. E-mail: sol.green@plantandfood.co.nz

Received 4 August 2011; Revised 4 November 2011; Accepted 7 November 2011

Abstract

Flowers of the kiwifruit species *Actinidia chinensis* produce a mixture of sesquiterpenes derived from farnesyl diphosphate (FDP) and monoterpenes derived from geranyl diphosphate (GDP). The tertiary sesquiterpene alcohol (*E*)-nerolidol was the major emitted volatile detected by headspace analysis. Contrastingly, in solvent extracts of the flowers, unusually high amounts of (*E*,*E*)-farnesol were observed, as well as lesser amounts of (*E*)-nerolidol, various farnesol and farnesal isomers, and linalool. Using a genomics-based approach, a single gene (*AcNES1*) was identified in an *A. chinensis* expressed sequence tag library that had significant homology to known floral terpene synthase enzymes. *In vitro* characterization of recombinant AcNES1 revealed it was an enzyme that could catalyse the conversion of FDP and GDP to the respective (*E*)-nerolidol and linalool terpene alcohols. Enantiomeric analysis of both AcNES1 products *in vitro* and floral terpenes *in planta* showed that (*S*)-(*E*)-nerolidol was the predominant enantiomer. Real-time PCR analysis indicated peak expression of *AcNES1* correlated with peak (*E*)-nerolidol, but not linalool accumulation in flowers. This result, together with subcellular protein localization to the cytoplasm, indicated that AcNES1 was acting as a (*S*)-(*E*)-nerolidol synthase in *A. chinensis* flowers. The synthesis of high (*E*,*E*)-farnesol levels appears to compete for the available pool of FDP utilized by AcNES1 for sesquiterpene biosynthesis and hence strongly influences the accumulation and emission of (*E*)-nerolidol in *A. chinensis* flowers.

Key words: *Actinidia*, farnesol, floral volatiles, kiwifruit, nerolidol, terpene, terpene synthase.

Introduction

Terpenes (also referred to as terpenoids or isoprenoids) represent the most abundant group of plant volatiles and are common components of floral scent and herbivore-induced volatile mixtures (Pichersky and Gershenzon, 2002; Shearer and Hampton, 2005; Dudareva and Pichersky, 2006). The volatility of plant terpenes enables them to act as chemical messengers that are received by organisms at different trophic levels. Terpenes not only underlie the complex communication system that exists between plants, pollinators, herbivores, and their parasites and predators (Unsicker *et al.*, 2009; Dicke and Baldwin, 2010), but ultimately serve to increase plant fitness (Harborne, 1991).

The diversity of terpene compounds in nature derives from the C5 compound isopentenyl diphosphate (IDP) and its allylic isomer dimethylallyl diphosphate (DMADP). Successive condensations of IDP with DMADP that proceed via the action of prenyltransferase enzymes, result in the formation of linear elongated prenyldiphosphates, including the C10 monoterpene precursor geranyl diphosphate (GDP), the C15 sesquiterpene precursor farnesyl diphosphate and the C20 diterpene precursor geranylgeranyl diphosphate (GGDP). In higher plants, the synthesis of IDP is compartmentally segregated (Lichtenthaler *et al.*, 1997) with the cytosolic mevalonate (MVA) pathway

(Goodwin, 1977; Nes and McKean, 1977; Spurgeon and Porter, 1981), supplying IDP for sesquiterpenoid production via farnesyl diphosphate (FDP), while the plastid-located MVA-independent or 2-C-methyl-D-erythritol-4-phosphate pathway (Eisenreich *et al.*, 1998; Lichtenthaler, 1999; Rohmer, 1999; Rodriguez-Concepcion and Boronat, 2002) produces IDP for mono- and di-terpenoid synthesis via GDP and GGDP, respectively. However, exchange of IDP, GDP, and/or FDP between the cytoplasmic and plastid compartments has also been observed (Adam and Zapp, 1998; Arigoni *et al.*, 1999; Hemmerlin *et al.*, 2003), while metabolic engineering in *Arabidopsis*, tobacco, and potato has shown the existence of low amounts of FDP in plastids and GDP in the cytosol (Aharoni *et al.*, 2003, 2006; Wu *et al.*, 2006).

Biosynthesis of terpenes is commonly restricted to specific plant tissues and specialized secretory structures contained within those tissues. Volatile terpenes are often emitted from specific floral tissues at particular times to attract pollinators. For example, Dudareva *et al.* (2003) demonstrated that the biosynthesis and emission of (*E*)-β-ocimene and β-myrcene in snapdragon (*Antirrhinum majus*) flowers correlated with specific expression patterns of the corresponding monoterpene synthase (TPS) genes in the upper and lower lobes of flower petals during floral development. The expression of these genes was also found to follow a weak diurnal cycle controlled by a circadian clock. Contrastingly, the expression of mono-TPS and sesqui-TPS enzymes in *Arabidopsis* flowers is limited to the stigma, anthers, nectaries, and sepals (Tholl *et al.*, 2005). The expression profiles of these TPS enzymes suggested that the volatile terpenes released from *Arabidopsis* flowers might both function as short-range attractants of pollinating insects and also provide a measure of defence for floral tissues vulnerable to microbial pathogens or herbivores.

The catalytic conversion of linear mono-, sesqui-, and di-terpene prenyldiphosphate compounds to terpenes is carried out by the TPS enzyme family. TPS biochemistry is generally characterized by electrophilically initiated reactions which, with the assistance of divalent metal ions, drive carbocation formation via ionization of the diphosphate precursor (Croteau, 1987; Cane, 1990; Lesburg *et al.*, 1998; Greenhagen and Chappell, 2001). Although TPS enzymes can produce a single compound with high regio- and stereospecificity (Croteau, 1987; Cane, 1990), they also show a propensity to generate multiple products from a single prenyldiphosphate substrate. In terms of floral terpene production, this is perhaps best illustrated in *Arabidopsis,* where only two enzymes were found to be responsible for the synthesis of the 20 identified sesquiterpenes (Tholl *et al.*, 2005).

To date, floral TPS enzymes have been identified and characterized in many flowering plants including *Arabidopsis*, *Clarkia,* snapdragon (Dudareva *et al.*, 1996; Dudareva *et al.*, 2003; Tholl *et al.*, 2005; Nagegowda *et al.*, 2008), and, more recently, in *Actinidia* species (Nieuwenhuizen *et al.*, 2009; Chen *et al.*, 2010). Characterized *Actinidia* TPS enzymes include those responsible for the predominant sesquiterpene volatiles (*E*,*E*)-α-farnesene and a (+)-germacreneD, produced by male and female *Actinidia deliciosa* flowers (Nieuwenhuizen *et al.*, 2009) and an (*S*)-linalool synthase, required for the production of floral lilac compounds in *Actinidia arguta* (Chen *et al.*, 2010).

In this study, we describe the identification and functional characterization of the enzyme responsible for the production of (*E*)-nerolidol that constitutes the major floral volatile in the commercially important kiwifruit species *Actinidia chinensis.* We also provide evidence that the formation of the dephosphorylated FDP derivative (*E*,*E*)-farnesol influences the capacity of *A. chinensis* to synthesize floral sesquiterpenes.

Materials and methods

Chemicals and chemical synthesis

2-Methyl-but-3-en-2-ol, 3-methyl-but-2-enol, (*E*)-hex-2-enol, rac-linalool, rac-(*E*,*Z*)-nerolidol, and (*E*,*E*)-farnesol were obtained from the Aldrich Chemical Company. (*S*)-Linalool and geranyllinalool were obtained from Fluka. Geraniol was from Acros Organics and geranylgeraniol was obtained from the Sigma Chemical Company. (*S*)-(*E*)-nerolidol was obtained from neroli essential oil (Neroli, *Citrus aurantium*, Lotus Essential Oils, Auckland, New Zealand). The essential oil (0.25 ml) was partially purified by flash chromatography on silica gel (pentane:DCM:-MeOH, 100:99:1) and (*E*)-nerolidol identified by GC-MS comparison with (*E*,*Z*)-nerolidol (Aldrich). Neroli contains exclusively (*E*)-nerolidol and predominantly (*S*)-(*E*)-nerolidol (Mondello *et al.*, 2002). Enantioselective GC-MS of the partially purified neroli essential oil determined it to be 14:86 (*R*):(*S*)-(*E*)-nerolidol.

8-Hydroxylinalool was synthesized according to a previously described method (Kreck *et al.*, 2002). Prenyldiphosphate substrates were synthesized by phosphorylation of the appropriate alcohols (Keller and Thompson, 1993), viz. DMADP from 3-methyl-but-2-enol, linalyl diphosphate (LDP) from rac-linalool, GDP from geraniol, (*E*,*E*)-FDP (FDP) from (*E*,*E*)-farnesol, and GGDP from geranylgeraniol. The isotopically-labelled substrates, [C1–$^3H_1$]-FDP and [C1–$^3H_1$]-GDP were made by phosphorylation of tritium-labelled farnesol and geraniol, respectively (Green *et al.*, 2007). The labelled alcohols were synthesized by MnO_2 or Dess-Martin periodinane (Comeskey *et al.*, 2004) oxidation of the appropriate alcohol to the aldehyde, then reduction (Croteau *et al.*, 1994) with NaB_3H_4 (Amersham).

Headspace volatile trapping and solvent extractions

A. chinensis Planch. var. chinensis ('Hort16A') flowers were harvested from the Plant & Food Research Actinidia orchard in Te Puke, New Zealand. Headspace volatiles were collected on site from whole flowers according to Matich *et al.* (2003) with minor modifications. Five fully opened flowers were harvested in triplicate every 4 h from noon (12:00 h on 18 October 2007) until 08:00 the following day. The harvested flowers were placed in 50 ml Quickfit tubes and the flower volatiles trapped for 3 h in direct thermal desorption tubes (ATAS GL International, Eindhoven, The Netherlands) packed with 80 mg Chromosorb absorbent (Shimadzu Co, Kyoto, Japan), using purified air at a flow rate of 25 ml min^{-1}.

Solvent extractions were carried out in triplicate on flowers samples (5 g) harvested at the equivalent time points to the headspace sampling. Flowers were transferred to 50 ml Quickfit tubes and extracted twice with 10 ml pentane:Et_2O (1:1 v/v) for 30 min with gentle shaking. The two extractions were combined and stored overnight at –20 °C. The following day the upper solvent layer was carefully removed from the lower frozen water layer using a glass pipette and reduced to 2 ml under a gentle stream of N_2. The concentrated extract was then passed through a column of anhydrous $MgSO_4$ to remove any remaining water.

Qualitative and semi-quantitative analysis of floral compounds

Headspace volatiles were desorbed directly from the thermal desorption tubes with a temperature ramp of 45–175 °C at 16 °C s^{-1} and cryofocused on the front of the capillary column by a liquid nitrogen-cooled cryogenic trap at –110 °C. After cryofocussing, the trap temperature was ramped to 175 °C at 50 °C min^{-1} (Optic 3 thermal desorption system, ATAS GL). A 15:1 split was employed while the volatiles were transferred into the capillary column at a column flow of 1 ml min^{-1}. The GC oven ramp was 35 °C for 2 min, 3 °C min^{-1} to 60 °C, 5 °C min^{-1} to 100 °C , 8 °C min^{-1} to 170 °C, 10 °C min^{-1} to 200 °C, and hold for 13 min. GC separations were on a 30 m × 0.25 mm i.d. × 0.25 μm film thickness DB-Wax (J & W Scientific, Folsom, CA, USA) capillary column in a HP6890 GC (Agilent Technologies) with helium as the carrier gas. The GC was coupled to a TOF-MS (Leco Pegasus III, St. Joseph, MI, USA). The ion source temperature was kept at 200 °C and ionization energy of 70 eV was used for electron impact ionization. The detector voltage was 1700 V, and ion spectra from 33 to 320 atomic mass units were collected with a data acquisition rate of 20 Hz. The total ion chromatograms were processed using the LECO ChromaTOF software.

Analysis of solvent extracted volatiles was carried out using the GC-MS system described above with the following modifications. Solvent extracts (1 μl) were injected into the GC with a 15:1 split and an injection port temperature of 200 °C. The GC oven ramp was 35 °C for 2 min, 3 °C min^{-1} to 60 °C, 5 °C min^{-1} to 100 °C, 8 °C min^{-1} to 190 °C, 10 °C min^{-1} to 230 °C, and hold for 15 min. The transfer line temperature was 220 °C.

Terpenes were identified using the following reference compounds: α-pinene, linalool, 1,8-cineole, and β-myrcene (Aldrich), limonene (BDH), β-pinene (K & K Laboratories), and sabinene (Phenomenex), Other compounds for which we did not have authentic standards (Tables 1 and 2) were identified by the ChromTOF software (version 2.3, Pegasus, Leco Australia) using the National Institute of Standards and Technology (NIST, version 2.0d, 2005) mass-spectral database, in combination with comparing the retention indices with those of a series of straight-chain hydrocarbon standards (C_8–C_{23}, 0.005 μl ml^{-1} for each hydrocarbon). Peaks were selected and integrated manually using the molecular ion and/or specific diagnostic ions of each compound. The terpenes were quantified by measuring m/z 93 peak areas against an average response factor for the m/z 93 peak areas of 1,8-cineole (0.0366 μl ml^{-1}), linalool (0.0263 μl ml^{-1}), and caryophyllene (0.03 μl ml^{-1}), contained in an external standard. Calibration curves determined that the GC-MS system gave a linear response, with respect to analyte concentration, over the range of concentrations for which they were measured in the headspace and in the solvent extracts.

Terpene glycoside extraction and analysis

Glycoside analysis was carried out according to previous methods (Young and Paterson, 1995) with minor modifications. Frozen flower tissue (2 g) was ground to a fine powder in liquid N_2, and transferred to a 50 ml Falcon tube and resuspended in 40 ml of water. The sample was centrifuged at 2000 *g* for 10 min at room temperature and the supernatant passed through a 15 mm × 25 mm i.d. Amberlite XAD-2 column (Supelco, Bellefonte, PA) according to the manufacturer's instructions. Bound glycosides were washed with 60 ml of water and the non-glycosylated compounds removed by the addition of Et_2O (40 ml). The bound glycosides were eluted with methanol (40 ml) and evaporated to dryness in a rotary evaporator. The resulting glycoside pellet was resuspended in 2.5 ml of de-glycosylation buffer (200 mM Na_2HPO_4 (pH 5), 220 mM citric acid) and re-extracted three times with 2.5 ml Et_2O. Enzymatic hydrolysis was carried out using Rapidase AR2000 (DSM Food Specialties, Delft, The Netherlands) which was dissolved in de-glycosylation buffer and used at a concentration of 2 mg ml^{-1}. The hydrolysis sample was overlaid with 500 μl of Et_2O and incubated for 24 h at 37 °C. Following the incubation, the sample was extracted a further three times with 1 ml of Et_2O. Prior to GC-MS analysis the pooled Et_2O extracts were passed through a column of anhydrous $MgSO_4$ and reduced to 1.5 ml.

Quantification was carried out on the DB-Wax GC column on the Waters-Agilent GC-MS system described above. Linalool (0.0001 μl ml^{-1}), 8-hydroxylinalool (0.00016 μl ml^{-1}), synthesized in-house according to the methods of Kreck *et al.* (2002), (*E*,*Z*)-nerolidol (0.0002 μl ml^{-1}), and (*E*,*E*)-farnesol (0.0002 μl ml^{-1}) were used as external authentic standards. A spike of 2 μl of 1 μl ml^{-1} of tridecane (Koch-Light) in each of the 1.5 ml standards (to give 0.00133 μl ml^{-1}) and c. 1.5 ml aglycone extracts was also used to correct for sample volumes and for GC-MS system responses, by correcting for the tridecane m/z 184 peak areas. Peak areas of the above terpenes were measured for m/z 93, and concentrations of the external standards were within an order of magnitude of those in the aglycone extracts, thus maintaining a linear response of the mass spectrometer over the concentrations of analytes in the different samples. Enantioselective GC-MS analysis of the linalool and (*E*)-nerolidol aglycones (data not shown) was performed on the Waters-Agilent GC-MS system and the β-Dex 325 GC column described above, using the oven temperature ramp employed for linalool.

Sequence analysis

Multiple amino acid sequence alignments of TPS genes were performed with Clustal X (Thompson *et al.*, 1997), using default parameters, and were manually adjusted in GeneDoc (www.nrbsc.org/gfx/genedoc/). Prediction of the AcNES1 protein open reading frame (ORF) was carried out using the EMBOSS (http://www.ch.embnet.org/EMBOSS/index.html) translation tool Transeq (Rice *et al.*, 2000). The bioinformatics tools ChloroP (Emanuelsson *et al.*, 1999) and TargetP (Emanuelsson *et al.*, 2000) available at http://www.cbs.dtu.dk/services/ were used to predict the intracellular targeting of AcNES1. Evolutionary relationships for TPS enzymes were inferred using the neighbour-joining method (Saitou and Nei, 1987). The evolutionary distances were computed using the Poisson correction method (Zuckerkandl and Pauling, 1965). Phylogenetic analyses were conducted in MEGA5.1 (Tamura *et al.*, 2007). The TPS accession numbers are given in Supplementary Table S1, available at *JXB* online.

Production of AcNES1 protein

An AcNES1 fragment possessing 5′ *Eco*RI and 3′ *Xho*I endonuclease sites was amplified by PCR from a 1978-bp *AcNES1* cDNA (GenBank accession JN242243) and cloned directly into the pET-30a expression vector (Novagen) as an *Eco*RI/*Xho*I fragment. Details of the primers are given in Supplementary Table S2. Recombinant proteins were expressed from the pET-30a plasmid following transformation into BL21-CodonPlus-RIL cells (Stratagene). Cultures (500 ml) were grown in ZYM-5052 autoinduction media (Studier, 2005) at 16 °C for 48–72 h at 300 rpm. Recombinant AcNES1 protein was extracted and purified according to previous methods (Green *et al.*, 2007). Eluted recombinant proteins were analysed by sodium dodecyl sulphate-polyacrylamide gel electrophoresis and terpene synthase activity measured. Protein concentrations were determined by Experion (BioRad) automated electrophoresis analysis, according to the manufacturer's instructions.

AcNES1 product analysis

AcNES1 solvent extraction assays for terpene product identification were carried out in 5 ml activity buffer (50 mM Bis-Tris propane (pH 7.5), 10 mM $MgCl_2$, and 5 mM DTT), in 50 ml glass tubes typically containing 50–100 μg purified recombinant AcNES1 protein and 20 μM FDP or GDP precursor. Assays were overlaid with 5 ml pentane:Et_2O (1:1 v/v) and incubated in a 30 °C water bath for 30 min. An additional 15 ml of solvent was added to each test tube and the tubes vortexed vigorously for 30 s to

extract the volatiles. The solvent extracts were dried using $MgSO_4$ and reduced in volume to 200 µl, under a stream of N_2, before GC-MS analysis.

GC-MS separations were carried out on an Agilent 6890N GC coupled to a Waters GCT ToF mass spectrometer. Initial chromatographic separations of 1 µl samples were on a 20 m × 0.18 mm i.d. × 0.18 µm film thickness DB-Wax (Agilent) capillary column with a He flow of 0.9 ml min^{-1} and an injection port temperature of 220 °C. The oven temperature ramp was 1 min at 35 °C, 5 °C min^{-1} to 240 °C, and hold for 15 min. The retention time and mass spectrum agreed with those of the authentic compounds obtained commercially and synthesized in-house. Enantioselective GC-MS separations were performed on the above GC-MS system on a 30 m × 0.25 mm i.d. × 0.25 µm film thickness β-Dex 325 (Supelco) capillary column with a helium flow rate of 1 ml min^{-1}. For analysis of AcNES1 products *in vitro* (after 1 µl, 1 min splitless injections), the oven temperature ramps were: 2-methyl-but-3-en-2-ol: 5 min at 28 °C and 5 °C min^{-1} to 230 °C: linalool: 1 min at 35 °C, 5 °C min^{-1} to 230 °C, and hold for 5 min; and (*E*)-nerolidol: 1 min at 50 °C, 3 °C min^{-1} to 130 °C, 7 °C min^{-1} to 230 °C, and hold for 10 min. For flower solvent extracts the oven temperature ramp for (*E*)-nerolidol and linalool was 1 min at 35 °C, 5 °C min^{-1} to 230 °C and hold for 5 min.

Enzyme kinetic analysis

Quadruplicate assays (50 µl) containing 50 mM BIS-TRIS propane (pH 7.5) and 150 nmoles AcNES1 protein were initiated by the addition of [C1–$^3H_1$]-FDP (4.0 GBq $mmol^{-1}$) or [C1–$^3H_1$]-GDP (6.2 GBq $mmol^{-1}$) precursors and incubated for 20 s at room temperature. Reactions were stopped with the addition of three volumes of 0.1M KOH/0.2 M EDTA solution and labelled products extracted with 0.5 ml pentane:Et_2O (1:1, v/v) and an aliquot taken for scintillation analysis. FDP and GDP kinetic determinations were carried out in the presence of 20 mM $MgCl_2$ or 20 mM $MnCl_2$ in separate assays. Cofactor determinations for Mg^{2+} and Mn^{2+} were carried out in the presence of 10 µM [C1–$^3H_1$]-FDP. Control assays using boiled enzyme were used to determine background radioactive counts. Kinetic constants were calculated from Bq data by non-linear regression of the Michaelis–Menten equation using the Origin 7.5 (Microcal Software. Northampton, MA, USA) graphics package. Data were calculated from three independent experiments.

Alternative substrate analysis

Relative velocity data (V_{rel}) for AcNES1 was also determined using prenyldiphosphates (50 µM) that were not tritium labelled, using semi-quantitative GC-MS. Assays were set up in the same manner as the 5 ml solvent extraction assay described above with the following exceptions: the duration of incubation was increased to 1 h and the enzyme concentration was decreased to 55 nmoles. For semi-quantitative GC-MS, sample peak areas were measured relative to authentic compounds (external standards) with tetradecane used as an internal standard in all samples to correct for day-to-day variation in the sensitivity of the GC-MS system. Enzyme activities were linear with time and enzyme concentration in all cases and were measured at least twice.

Real-time gene expression analysis

RNA was extracted from flowers, flower parts, fruit, and leaves according to Nieuwenhuizen *et al.* (2007) and treated with 10 U of DNaseI (Roche Applied Science, Mannheim, Germany) before cDNA synthesis. First-strand cDNA was synthesized using the Transcriptor First Strand cDNA Synthesis Kit (Roche) according to the manufacturer's instructions and diluted 50-fold before use. Relative quantitation real-time gene expression analysis of targets and the housekeeping gene elongation factor 1α were performed (four technical replicates) on a LightCycler 480 platform using the LightCycler 480 SYBR Green master mix and results were analysed using the LightCycler 480 software (Roche). The analysis was carried out using the –ΔCp method according to Montefiori *et al.*, (2011), enabling a comparison of the level of expression of multiple target genes normalized to a common reference gene considered stable and unchanging in the different samples. The thermal programme was 5 min at 95 °C and 40 cycles of 10 s at 95 °C, 10 s at 60 °C, and 20 s at 72 °C, followed by melting curve analysis at 95 °C 5 s and 65 °C 60 s, and then ramping at 0.18 °C s^{-1} to 95 °C. Primers for real-time gene expression analysis are listed in Supplementary Table S2.

Transient expression and subcellular targeting

In planta transient expression was carried out according to the methods of Nieuwenhuizen *et al.* (2009) utilizing the *Agrobacterium tumefaciens* strain GV3101 harbouring the pHEX2 binary vector (Hellens *et al.*, 2005). For transient expression vector construction, AcNES1 was amplified by PCR using universal primers (Hellens *et al.*, 2005) and cloned into the pHEX2 binary vector.

For the AcNES1 subcellular targeting analysis, an in-frame N-terminal green fluorescent protein (GFP) fusion was constructed according to the methods of Nieuwenhuizen *et al.* (2009). Primers for the *AcNES1* PCR amplification step are listed in Supplementary Table S2. The amplified DNA was digested with *Bam*HI and *Xba*I and cloned into the p326-SGFP vector (Lee *et al.*, 2001), culminating in the p326-AcNES1/SGFP vector.

Results

Volatile emission and accumulation in A. chinensis flowers

The emission of floral terpenes by *A. chinensis* was investigated using a combination of dynamic headspace sampling and solvent extraction followed by GC-MS analysis. Volatile sampling, which was carried out over the course of a 24 h day/night cycle, revealed a mixture of monoterpenes, sesquiterpenes, and various terpene derivatives to be present in the headspace of the flowers (Table 1). (*E*)-nerolidol emission, calculated on a ng (g fresh weight)$^{-1}$ h^{-1} (gFW^{-1} h^{-1}) basis over a day/night cycle, constituted ~30% of the total emitted terpenes and was produced at an average rate of 7.5 ng gFW^{-1} h^{-1}. The (*E*,*E*)-α-farnesene oxidation product, 6-methyl-5-hepten-2-one (Anet, 1972), was the second most prevalent terpene compound, with an emission rate of ~4.18 ng gFW^{-1} h^{-1}, while (*E*,*E*)-α-farnesene emission was the next highest, at ~1.15 ng gFW^{-1} h^{-1}. Lower amounts of the terpene metabolites (*E*)- and (*Z*)-geranyl acetone and 4,8-dimethyl^{-1},3,7-nonatriene, which were assumed to be oxidative degradation products of (*E*)-nerolidol (Donath and Boland, 1995; Boland *et al.*, 1998), were also present. The emission profiles for the main floral sesquiterpenes (Fig. 1) showed that peak (*E*)-nerolidol emission occurred at midnight (0:00 h) then declined over the next 8 h where it remained low until evening. Although there was a suggestion of smaller day-time (*E*)-nerolidol emission peak at 16:00 h, the emission rates between noon and 20:00 h were not significantly different. The emission profile for (*E*,*E*)-α-farnesene and its oxidation product 6-methyl-5-hepten-2-one remained relatively constant, although levels did appear to gradually decline from

Table 1. *Actinidia chinensis* flower semi-quantitative headspace terpene analysis

Emission rates for individual terpenes (listed in order of concentration) are calculated on the average hourly emission over a 24 h day/night cycle and are presented as ng (g fresh weight)$^{-1}$ h^{-1}. Fractions are given as a percentage of total emitted terpenes. Sums for each terpene class are italicized.

Compound	Concentration	Fraction
Sesquiterpenes		
(*E*)-Nerolidol	7.50	29.90
(*E*,*E*)-Farnesal	1.30	5.18
(*E*,*E*)-α-Farnesene	1.15	4.58
(*Z*,*E*)-Farnesal	0.93	3.71
(*E*,*E*)-Farnesol	0.26	1.04
(*Z*,*E*)-α-Farnesene	0.14	0.56
(*Z*,*E*)-Farnesol	0.03	0.12
Total	*11.31*	*45.1*
Monoterpenes		
(*E*)-β-Ocimene	1.55	6.18
Linalool	1.46	5.82
α-Pinene	1.40	5.58
Sabinene	1.07	4.27
β-Pinene	0.72	2.87
1,8-Cineole	0.64	2.55
(*Z*)-β-Ocimene	0.51	2.03
Limonene	0.37	1.47
β-Myrcene	0.27	1.00
α-Thujene	0.22	0.88
Total	*8.21*	*32.73*
Terpene metabolites		
6-Methyl-5-hepten-2-one[a]	4.18	16.62
(*E*)-Geranyl acetone[a]	0.73	2.90
4,8-Dimethyl-1,3,7-nonatriene[b]	0.63	2.51
(*Z*)-Geranyl acetone[b]	0.02	0.09
Total	*5.56*	*22.17*

[a] Oxidative breakdown product (*E*,*E*)-α-farnesene (Anet, 1972).
[b] Oxidative breakdown products of nerolidol (Donath and Boland, 1995; Boland *et al*., 1998).

midnight onwards. Generally, the concentrations of the different monoterpenes (Supplementary Fig. S1) were low (< 3 ng gFW^{-1} h^{-1}) and showed little variation over the course of the day/night cycle, although cumulative amounts of monoterpenes and sesquiterpenes (predominantly (*E*)-nerolidol) were similar (Table 1).

Solvent extractions of flowers taken at the equivalent time points to the above headspace analysis were analysed for the presence of accumulated volatiles. In contrast to the emitted volatiles, the profile of accumulated volatiles was significantly less complex and primarily consisted of sesquiterpenes (Table 2). On a whole-flower fresh-weight basis, the dephosphorylated FDP derivative (*E*,*E*)-farnesol was by far the most prevalent compound occurring at ~18,700 ng gFW^{-1}, or ~72%, of the total extracted terpene volatiles. The accumulated terpenes, presumed to be produced by TPS enzymes, were dominated by linalool and (*E*)-nerolidol, with ~1500 and ~890 ng gFW^{-1} respectively. Time point analysis of these terpenes (Fig. 2) showed that (*E*,*E*)-farnesol and

Table 2. *Actinidia chinensis* flower semi-quantitative solvent-extracted terpene analysis Terpenes are listed in order of concentration and are presented as ng (g fresh weight)$^{-1}$ h^{-1}. Fractions are given as a percentage of total accumulated terpenes.

Compound	Concentration	Fraction
Sesquiterpenes		
(*E*,*E*)-Farnesol	18700	72.4
(*E*,*E*)-Farnesal	1600	6.2
(*Z*,*E*)-Farnesol	1070	4.1
(*E*)-Nerolidol	890	3.4
(*Z*,*E*)-Farnesal	820	3.2
(*E*,*Z*)-Farnesol	580	2.2
Monoterpenes		
Linalool	1500	5.8
Geraniol	400	1.5
Geranyl acetate	280	1.1

(*E*)-nerolidol were largely accumulated during the day, with peak concentrations occurring at noon. Notably, the highest concentrations of accumulated (*E*)-nerolidol corresponded to the lowest rate of emitted (*E*)-nerolidol and *vice versa*, while linalool accumulation remained relatively constant over the course of the day/night cycle.

Volatile glycosylation in A. chinensis *flowers*

Differences in the accumulation and emission patterns for (*E*)-nerolidol and (*E*,*E*)-farnesol in *A. chinensis* flowers suggested that these compounds might be sequestered in non-volatile glycosylated form for later release. Floral glycosides were extracted from *A. chinensis* and analysed by GC-MS after enzymatic hydrolysis (Fig. 3). This analysis showed that glycosylated forms of (*E*)-nerolidol, (*E*,*E*)-farnesol, and linalool were present in the flowers, as well as high levels of glycosylated 8-hydroxylinalool. Glycosylated (*E*)-nerolidol was detected at midnight, at ~290 ng gFW^{-1} (or ~44% of the total (*E*)-nerolidol pool), and increased to 340 ng gFW^{-1} at noon (although this level now only equated to ~12% of the total (*E*)-nerolidol pool). There was no glycosylated (*E*)-nerolidol detected following the period of peak (*E*)-nerolidol accumulation at noon (Fig. 2), suggesting that between noon and 16:00 h the sequestered (*E*)-nerolidol had been remobilized and released from the flower. The pattern of (*E*,*E*)-farnesol glycosylation (Fig. 3B) was similar to that of (*E*)-nerolidol, although it only comprised a minor component (~0.1–6%) of the total (*E*,*E*)-farnesol pool. Glycosylated linalool accounted for between ~2.5% and 6.5% of the total linalool pool with peak accumulation occurring between midnight and noon. Unexpectedly, 8-hydroxylinalool (Fig. 3C), was by far the most predominant *A. chinensis* glycosylated floral terpene, with levels declining from ~87% (~11,300 ng gFW^{-1}) of the total linalool pool at midnight to 62 % (~2600 ng gFW^{-1}) at 20:00 h.

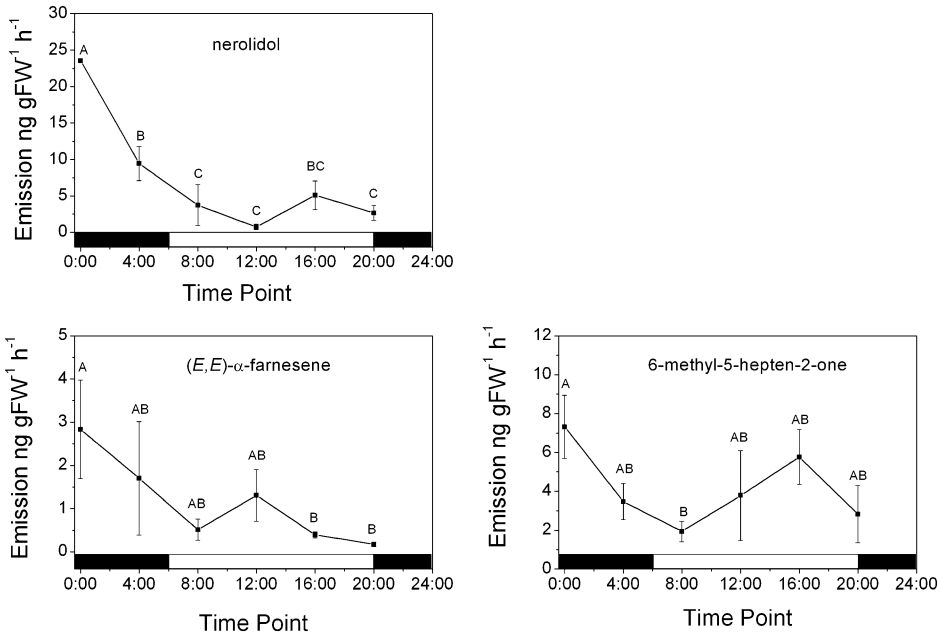

Fig. 1. Rates of sesquiterpene and homoterpene release from *A. chinensis* flowers during a day/night cycle. Terpene volatiles were trapped from triplicate flower samples by dynamic headspace sampling at 4-h intervals and analysed by GC-MS. Data are presented as mean ± SEM ($n = 3$). Means labelled without a common letter are significantly different ($P < 0.05$) based on LSD of one-way ANOVA.

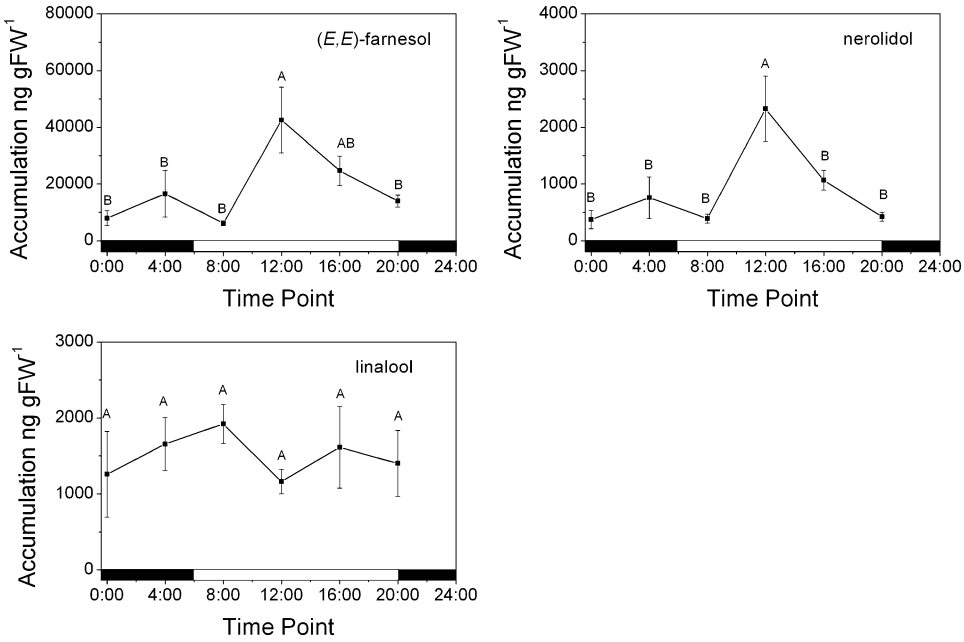

Fig. 2. Rates of sesquiterpene and monoterpene accumulation in *A. chinensis* flowers during a day/night cycle. Terpene volatiles were solvent extracted at 4-h intervals over the course of 24 h. Data are presented as mean ± SEM ($n = 3$). Means labelled without a common letter are significantly different ($P < 0.05$) based on LSD of one-way ANOVA.

Identification of terpene synthase-like sequences from A. chinensis *flowers*

A homology-based gene mining approach was taken to identify putative TPS enzymes that could account for the production of the terpene compounds identified in *A. chinensis* flowers. A search of an *Actinidia* expressed sequence tag database (Crowhurst *et al.*, 2008) identified a single contig from floral tissue with sequence homology to known floral TPS sequences (Supplementary Fig. S2). This transcript represented a full-length cDNA (termed AcNES1) of 1978 nucleotides encoding a predicted protein of 573 amino acids and ~65.4 kDa. AcNES1 was not predicted to contain a plastid-targeting peptide according to the ChloroP and TargetP prediction programmes. Phylogenetic analysis showed that AcNES1 clustered in a well-supported manner with the TPS enzymes in the TPS-g subgroup (Bohlmann *et al.*, 1998; Dudareva *et al.*, 2003) (Fig. 4). The TPS-g enzymes are

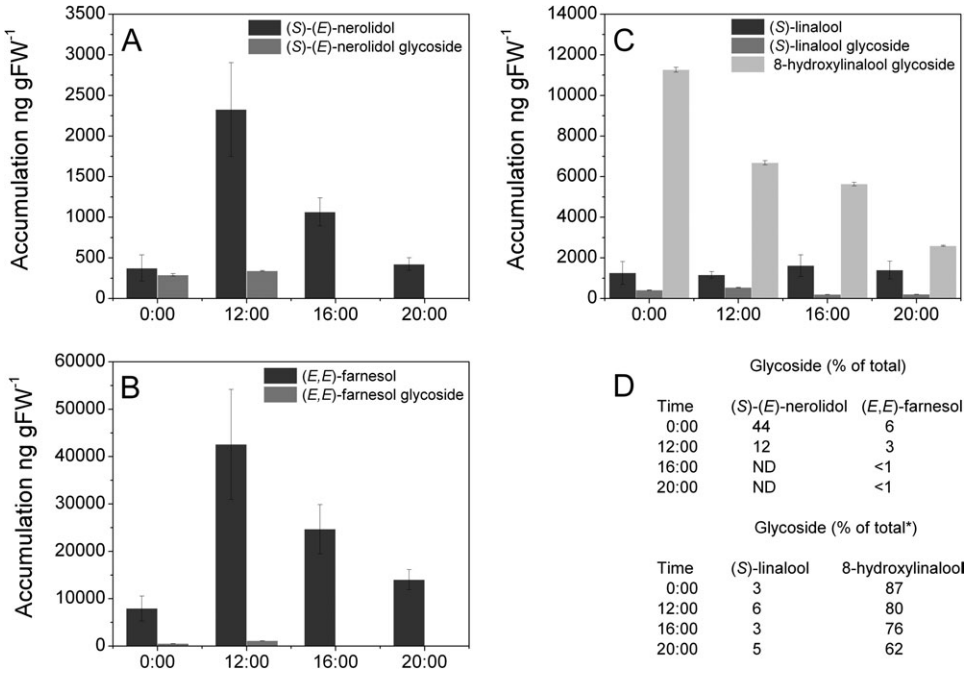

Fig. 3. Analysis of glycosylated terpenes in *A. chinensis* flowers. Glycosylated terpenes were extracted from flower tissue harvested at four time points during a day/night cycle and enzymically hydrolysed to release the corresponding aglycones. (A–C) Levels of glycosylated (*S*)-(*E*)-nerolidol (A), (*E*,*E*)-farnesol (B), and (*S*)-linalool (C) shown in comparison with non-glycosylated levels taken from Fig. 2. (D) Glycosylated terpenes given as a percentage of total terpenes. * Total linalool includes the 8-hydroxylinalool component. ND, not detected. Data are presented as mean ± SEM ($n = 3$).

characterized by the absence of an N-terminal RRX_8W motif, which is reported to be essential for cyclic monoterpene production in the angiosperm TPS-b and gymnosperm TPS-d enzyme subgroups (Savage *et al.*, 1994). AcNES1 was most similar to the *Actinidia polygama* and *A. arguta* linalool synthases (Chen *et al.*, 2010), with ~78% amino acid identity.

Enzymatic properties of AcNES1

Purified recombinant AcNES1 protein was analysed for activity with GDP and FDP precursors in separate solvent extraction assays (Fig. 5). GC-MS analysis of the pentane/Et_2O extracted volatiles showed that AcNES1 could catalyse the conversion of both FDP and GDP precursors to the respective terpene alcohols (*E*)-nerolidol and linalool. The smaller amount of (*Z*)-nerolidol produced by AcNES1 was assumed to derive from (*Z*,*E*)-FDP contamination of the (*E*,*E*)-FDP used. Kinetic evaluation of recombinant AcNES1 enzyme (Table 3) showed that it had a higher binding affinity for FDP compared with GDP (K_m values of 0.80 and 1.89 μM respectively) and an approximate four-fold increase in catalytic efficiency (k_{cat}/K_m) in the presence of FDP (300 s^{-1} mM^{-1}) compared with GDP (69 s^{-1} mM^{-1}). AcNES1 also showed an approximate 8-fold increase in its affinity for Mn^{2+} ($K_m \approx 14.2$ μM compared with Mg^{2+} ($K_m \approx 117$ μM) as the divalent metal cofactor. However, in the presence of Mn^{2+} AcNES1, activity was only ~22% of that observed with FDP and Mg^{2+} together and ~54% of that observed with GDP and Mg^{2+} together. The kinetics for substrate and divalent metal ion preference are similar to those observed for other TPS-g enzymes (Nagegowda *et al.*, 2008; Chen *et al.*, 2010).

Enantiomeric analysis of terpene compounds from AcNES1 and A. chinensis *flowers*

Enantioselective GC-MS analysis of (*E*)-nerolidol and linalool produced by AcNES1 determined that (*S*)-(*E*)-nerolidol and (*S*)-linalool (Fig. 6) were the predominant enantiomers. AcNES1 was also observed to produce (*S*)-linalool (Fig. 6F) from racemic LDP, while the small amount of (*R*)-linalool observed was assumed to have derived from LDP breakdown. This assumption was based on the fact that other racemic monoterpene products were seen in this analysis (data not shown). Equivalent analysis of an *A. chinensis* whole-flower extract (Fig. 6D) also showed that (*S*)-(*E*)-nerolidol was the predominant enantiomer and hence supports the assumption that AcNES1 is likely to be responsible for floral (*S*)-(*E*)-nerolidol biosynthesis in *A. chinensis*. In contrast to the (*S*)-linalool produced by AcNES1, the predominant linalool enantiomer in *A. chinensis* flowers, as previously shown by Matich *et al.* (2010) was (*R*)-linalool.

Alternative substrate usage by AcNES1

The sequence homology of AcNES1 to TPS-g nerolidol/linalool and linalool/nerolidol/geranyllinalool synthases from grape (Martin *et al.*, 2010) provided a rational basis for testing additional prenyldiphosphate substrates ranging from C5 to C20. This analysis (summarized in Table 4)

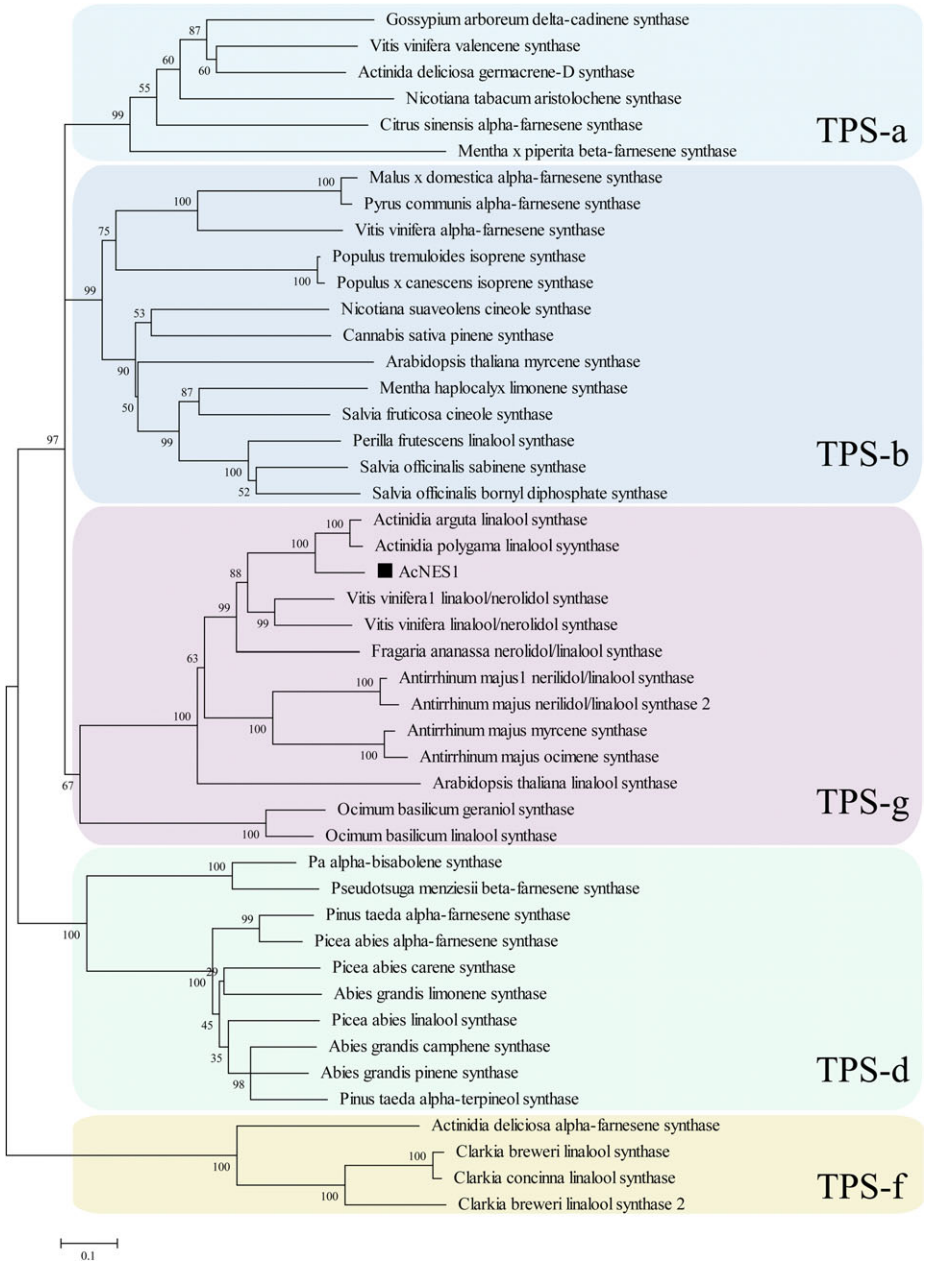

Fig. 4. Phylogenetic analysis of selected plant terpene synthase (TPS) enzymes. The clusters correspond to the previously recognized TPS subfamilies (TPS-a -TPS-g) (Bohlmann *et al*., 1998; Dudareva *et al*., 2003). Terpene synthases from the TPS-e and TPS-c subgroups, which are involved in plant primary metabolism, were not included in this analysis. AcNES1 is indicated by a filled square. Protein alignments were conducted using the ClustalX algorithm and trees were inferred using the neighbour-joining method. $N =$ 10,000 replicates for bootstrapping. Accession numbers for each enzyme are given in Supplementary Table S1.

showed that AcNES1 was able to catalyse the conversion of GGDP (C20) to the corresponding terpene alcohol geranyllinalool at ~10% of the optimized rate for (*E*)-nerolidol from FDP but was unable to convert the C5 hemiterpene (isoprene) precursor DMADP to its corresponding alcohol. This *in vitro* plasticity for GDP, FDP and GGDP prenyldiphosphate usage in AcNES1 is mirrored in the activity of the three grape TPS-g sesqui-TPS enzymes (Martin *et al.*, 2010) and again demonstrates an inherent capacity for TPS enzymes to evolve different product and substrate specificities.

Gene expression analysis

Relative gene expression analysis was carried out to investigate the spatial and temporal regulation patterns of *AcNES1* expression in *A. chinensis* (Fig. 7). The highest *AcNES1* expression was observed in the petals of fully open flowers, with lower expression in the stamens and pistils (Fig. 7A). *AcNES1* expression was not observed in unopened flowers. Over the course of a day/night cycle, *AcNES1* expression followed a weak diurnal rhythm with peak

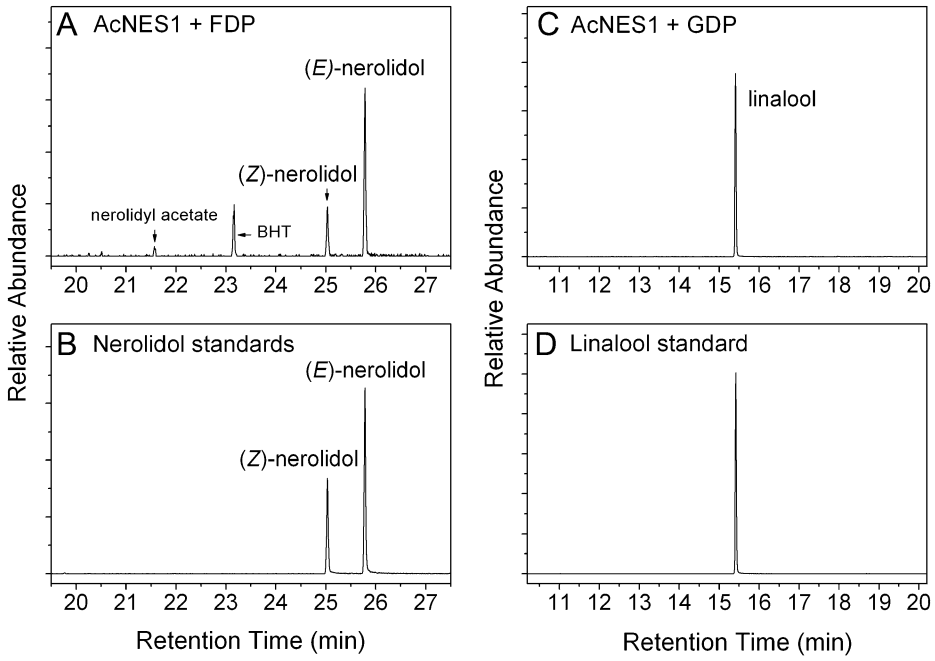

Fig. 5. AcNES1 GC-MS analysis. (A) Pentane/Et_2O samples extracted from assays containing purified recombinant AcNES1 in the presence of FDP. (B) Authentic (*Z*)- and (*E*)-nerolidol standards. (C) Linalool produced by AcNES1 from GDP. (D) Authentic linalool standard. The butylhydroxytoluene contaminant seen in (A) is derived from the diethyl ether used in the terpene volatile extraction.

Table 3. Kinetic profiles of recombinant AcNES1 protein
Recombinant AcNES1 enzyme was obtained using a combination of Ni^{2+} affinity and gel filtration chromatography. Kinetic parameters are given for both farnesyl diphosphate (FDP) and geranyl diphosphate (GDP) (0.25–100 μM) in the presence of 20 mM $MgCl_2$. FDP and GDP kinetic determinations in the presence of $MnCl_2$ were not calculated due to the low activity rates of AcNES1 with the Mn^{2+} cation. Kinetic parameters are also given for Mg^{2+} (0.05–20 mM) and Mn^{2+} (0.01–2.5 mM) in the presence of 10 μM FDP. K_m, Michaelis constant. All values represent mean ± SE ($n = 3$). AcNES1 turnover rates (k_{cat}) were calculated under conditions of saturating substrate and divalent metal ion concentrations. Relative velocity (V_{rel}) data were determined from k_{cat} values. NA, not applicable.

	K_m (μM)	k_{cat} (s^{-1})	k_{cat}/K_m (s^{-1} mM^{-1})	V_{rel} (%)
FDP (Mg^{2+})	0.80 ± 0.26	0.24 ± 0.013	300	100
Mg^{2+} (FDP)	117 ± 37			
Mn^{2+} (FDP)	14.2 ± 2.70	0.053 ± 0.005		22
GDP (Mg^{2+})	1.89 ± 0.20	0.13 ± 0.002	69	54
GDP (Mn^{2+})	NA	0.03 ± 0.003		12

expression levels occurring between 20:00–0:00 h and 8:00–12:00 h (Fig. 7B).

Gene expression analysis was also carried out to determine how genes in the MVA pathway might modulate FDP flux and consequently sesquiterpene emission and/or accumulation in *A. chinensis* flowers (Fig. 8). The profiles of three family members encoding the key regulatory enzyme HMG-CoA reductase (HMGR) (Maurey *et al.*, 1986; Gondet *et al.*, 1992; Hemmerlin *et al.*, 2003; Hey *et al.*, 2006; Muñoz-Bertomeu *et al.*, 2007) and the mevalonate-5-diphosphate decarboxylase gene (*MDC*) peaked in expression at 08:00 h. This peak in expression preceded maximal (*E*,*E*)-farnesol and (*E*)-nerolidol accumulation at noon (Fig. 2), and suggests a link between FDP substrate flux and sesquiterpene accumulation in *A. chinensis* flowers. Interestingly, the reduction of floral *HMGR* gene expression between 08:00 h and noon also coincided with increasing (*E*,*E*)-farnesol concentrations (Figs. 8 and 2, respectively). Expression analysis for the other MVA genes (Fig. 8) showed that peak expression for the 3-hydroxy-3-methylglutaryl-CoA synthase (*HMGS*), phosphomevalonate kinase (*PMK*), and isopentenyldiphosphate isomerase (*IDPI*) genes all occurred at 20:00 h.

Subcellular localization and in planta activity of AcNES1

The subcellular localization of AcNES1 was investigated using an AcNES1-GFP fusion protein in *Arabidopsis* protoplasts. Confocal laser scanning microscopy (Fig. 9) revealed a diffuse GFP fluorescence pattern for AcNES1-GFP protein distribution exclusively present in the cytosol. Similar fluorescence patterns were observed for a control GFP expression product, while no fluorescence was observed in untransfected protoplasts. These results are in agreement with the lack of a predicted AcNES1 plastid-targeting signal (ChloroP) and confirm that this enzyme is located in the cytosol.

A. tumefaciens-mediated transient expression (Hellens *et al.*, 2005) in *Nicotiana benthamiana* leaves was used to confirm that AcNES1 acted as a (*E*)-nerolidol synthase *in planta*. *N. benthamiana* leaves infiltrated with a CaMV 35S-driven binary *AcNES1* vector construct produced significant

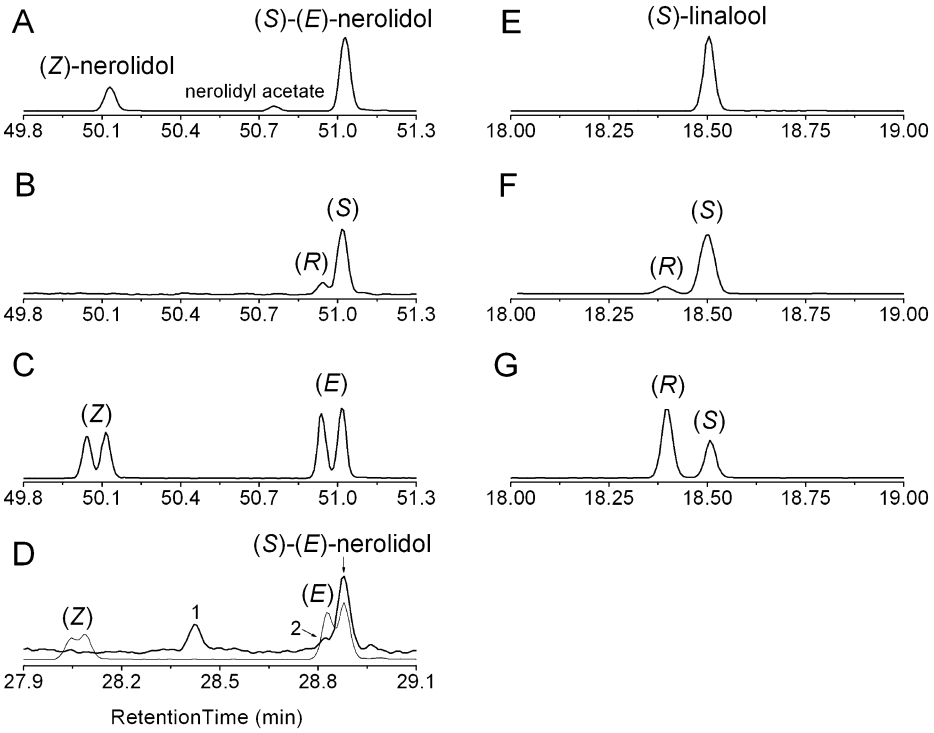

Fig. 6. Enantioselective analysis of AcNES1 terpene synthase activity. (A) GC-MS profile (m/z 93) for AcNES1 activity in the presence of FDP. (B) Profile (m/z 93) for a neroli standard showing (*R*)-(*E*)-nerolidol and (*S*)-(*E*)-nerolidol peaks. (C) Total ion current GC-MS profile for nerolidol standard (Aldrich) showing (*Z*)-nerolidol and (*E*)-nerolidol peaks. (D) Comparative GC-MS profile for whole-flower extract (black line) with nerolidol standard (grey line); a non-terpene peak (1) and small (*R*)-(*E*)-nerolidol peak (2) are also indicated. (E) AcNES1 with GDP. (F) Racemic linalyl diphosphate. (G) Control GC-MS trace (m/z 93) for a racemic and (*R*)-linalool standard. A faster ramp rate was used in (D).

Table 4. Semi-quantitative GC-MS analysis of AcNES1 alternate substrate usage

FDP, Farnesyl diphosphate; GDP, geranyl diphosphate; GGDP, geranylgeranyl diphosphate; LDP, linalyl diphosphate.

	Relative velocity (V_{rel} %)			
Product (%)	**LDP**	**GDP**	**FDP**	**GGDP**
(*R*)-Linalool	0.7			
(*S*)-Linalool	2.2	58.4		
(*S*)-(*E*)-Nerolidol			100[a]	
Geranyl linalool				10.3

[a] 100% = k_{cat} ~0.127 s^{-1}.

amounts of nerolidol (Fig. 10). (*E*)-nerolidol was not produced in control *N. benthamiana* leaves that had been infiltrated with buffer or a GUS-containing binary vector. Small amounts of linalool were also identified in both the control and *AcNES1* infiltrated leaves and were therefore assumed to be derived from an endogenous linalool synthase.

Discussion

Terpene emission by *A. chinensis* flowers is dominated by the tertiary sesquiterpene alcohol (*E*)-nerolidol. (*E*)-nerolidol is a common volatile constituent of plants and nerolidol synthases have been characterized in a number of plant species including strawberry (Aharoni *et al.*, 2004), grape (Martin *et al.*, 2010), snapdragon (Nagegowda *et al.*, 2008), and maize (Schnee *et al.*, 2002). (*E*)-nerolidol is likely to play a role in attracting pollinators or seed dispersal agents and is also produced by plants in response to insect herbivory (Bouwmeester *et al.*, 1999; Degenhardt and Gershenzon, 2000; Danner *et al.*, 2011). Our data shows that, in *A. chinensis*, (*E*)-nerolidol mostly accumulates during the day, while its release occurs mostly during the night (Figs. 1 and 2, respectively). This not only contrasts to the emission of (*E*)-nerolidol in snapdragon flowers (Dudareva *et al.*, 2005) and (*E*,*E*)-farnesene and germacrene-D in *A. deliciosa* (Nieuwenhuizen *et al.*, 2009), which occurs during the day, but also suggests a possible role in attracting night-time insect pollinators.

One feature that differentiates *A. chinensis* floral terpene metabolism from that of other kiwifruit species is the low rates of floral terpene emission. Peak (*E*)-nerolidol emission in *A. chinensis* is more than 3-fold lower than the equivalent (*E*,*E*)-α-farnesene emission in *A. deliciosa* (i.e. ~24 v. 76 ng gFW^{-1} h^{-1}, respectively) (Nieuwenhuizen *et al.*, 2009), while total monoterpene emissions in *A. chinensis* (~8.2 ng gFW^{-1} h^{-1}) equate to only ~9% of the linalool emission in *A. arguta* (Chen *et al.*, 2010). Although the level of

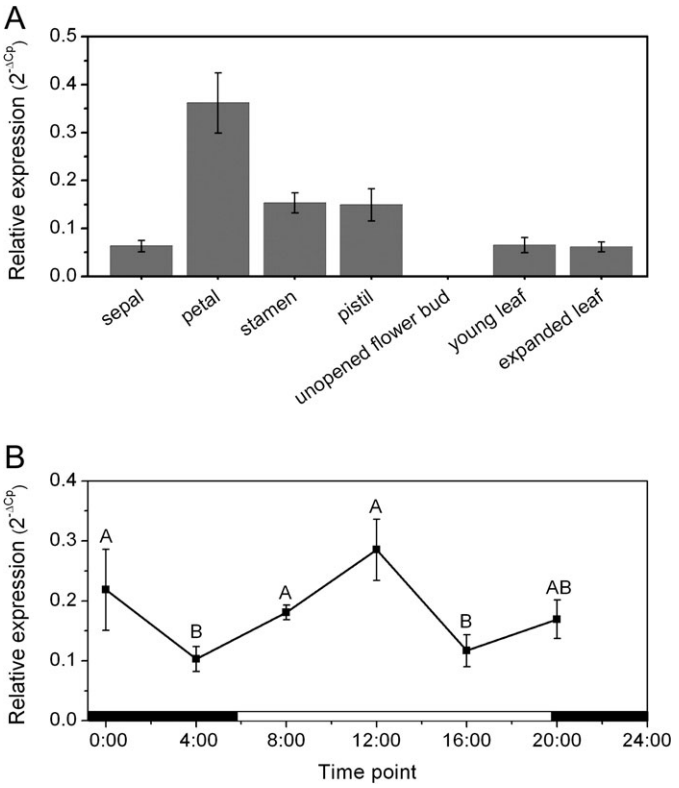

Fig. 7. Relative gene expression analysis of *AcNES1* in *A. chinensis*. *AcNES1* expression levels were determined in floral and vegetative tissue (A) and in whole flowers during a 24 h day/night cycle (B). The data were analysed using the target/reference ratio calculated with the LightCycler 480 software, enabling a comparison of the level of expression of different gene family members compared to the reference gene *EF1α*, considered stable and unchanging in the different tissues during development. Primer efficiencies were between 1.96 and 2.0. Data are presented as mean ± SEM ($n = 4$). Means labelled without a common letter are significantly different ($P < 0.05$).

accumulated linalool in *A. chinensis* flowers appears to be higher than that observed for *A. arguta* (1.5 μg gFW^{-1} versus 0.1 μg gFW^{-1} respectively), linalool turnover in *A. arguta* flowers is likely to be significantly higher. The linalool produced in *A. arguta* flowers has many highly abundant biosynthetic derivatives (Chen *et al.*, 2010), which would be expected to deplete the pool of accumulated linalool.

Terpene volatile sequestration in A. chinensis *flowers*

The apparent disconnect between the accumulation and emission of (*E*)-nerolidol suggested that sequestration might be involved in regulating levels of terpene volatiles in *A. chinensis* flowers. However, our analysis showed that the glycosylation profile cannot account for the difference in the timing of (*E*)-nerolidol production and release. A significant proportion of the total (*E*)-nerolidol pool (44%) was glycosylated at midnight (Fig. 3A and D), which corresponded to the time of peak of (*E*)-nerolidol emission (Fig. 1) rather than accumulation as might be expected. Moreover, during the peak accumulation of (*E*)-nerolidol at noon and then during its steady decline from noon to 20:00 h, glycosylated (*E*)-nerolidol was not detected.

Interestingly, glycosylation is likely to be impacting on floral linalool emission in *A. chinensis*. Significant amounts of linalool are produced (Fig. 3C and D); however, the majority is either glycosylated directly or enzymatically converted to 8-hydroxylinalool and then glycosylated. The presence of 8-hydroxylinalool has also been observed as an unexpected consequence of over-expressing a *Clarkia* (*S*)-linalool synthase in tomato (Lewinsohn *et al.*, 2001) and was put down to the presence of a hydroxylase able to act on (*S*)-linalool.

The function of AcNES1 in A. chinensis *flowers*

Subcellular protein localization can control terpene biosynthesis *in planta* by modulating terpene precursor accessibility. Although it is generally accepted that GDP and FDP biosynthesis are segregated to plastidial and cytosolic compartments, respectively, low concentrations of plastidial FDP and cytosolic GDP have been identified in *Arabidopsis*, tobacco, and potato (Aharoni *et al.*, 2003, 2006; Wu *et al.*, 2006). It is therefore possible that an enzyme that shows bifunctional behaviour *in vitro* can also exhibit the same behaviour *in planta*. This appears to be true for the bifunctional, cytosolically targeted FaNES1 enzyme in strawberry, which is reported to synthesize both (*E*)-nerolidol and linalool in cultivated strawberry fruit (Aharoni *et al.*, 2004). However in *Antirrhinum majus* flowers, the bifunctional cytosolically-targeted AmNES/LIS1 enzyme has been shown to produce (*E*)-nerolidol exclusively from cytoplasmic FDP pools, whilst the chloroplast-targeted AmNES/LIS2 enzyme exclusively produces linalool from plastid (specifically leucoplasts) GDP pools (Nagegowda *et al.*, 2008). The cytosolically targeted AcNES1 enzyme from *A. chinensis* flowers is also likely to act exclusively as a (*E*)-nerolidol synthase, as *N. benthamiana* leaves transiently over-expressing *AcNES1* (Fig. 10) produced only (*E*)-nerolidol. Two additional results support the contention that AcNES1 acts as an (*S*)-(*E*)-nerolidol synthase and not a linalool synthase in *A. chinensis* flowers. The (*S*)-(*E*)-nerolidol enantiomer produced by AcNES1 matches the predominant floral (*E*)-nerolidol enantiomer (Fig. 6A and D, respectively) and AcNES1 produces (*S*)-linalool from GDP, not (*R*)-linalool as found in flowers.

Regulation of terpene biosynthesis in A. chinensis *flowers*

An unusual feature of *A. chinensis* flowers is the high amounts of (*E*,*E*)-farnesol that they accumulate (Table 2) compared with flowers from other species, including other kiwifruit (Matich *et al.*, 2003; Crowhurst *et al.*, 2008). It is also notable that the delicate floral tissue is not adversely affected by (*E*,*E*)-farnesol concentrations that can reach 42,600 ng gFW^{-1} (or ~190 μM), considering that 25 μM is reported to be toxic to tobacco BY-2 cells (Hemmerlin and

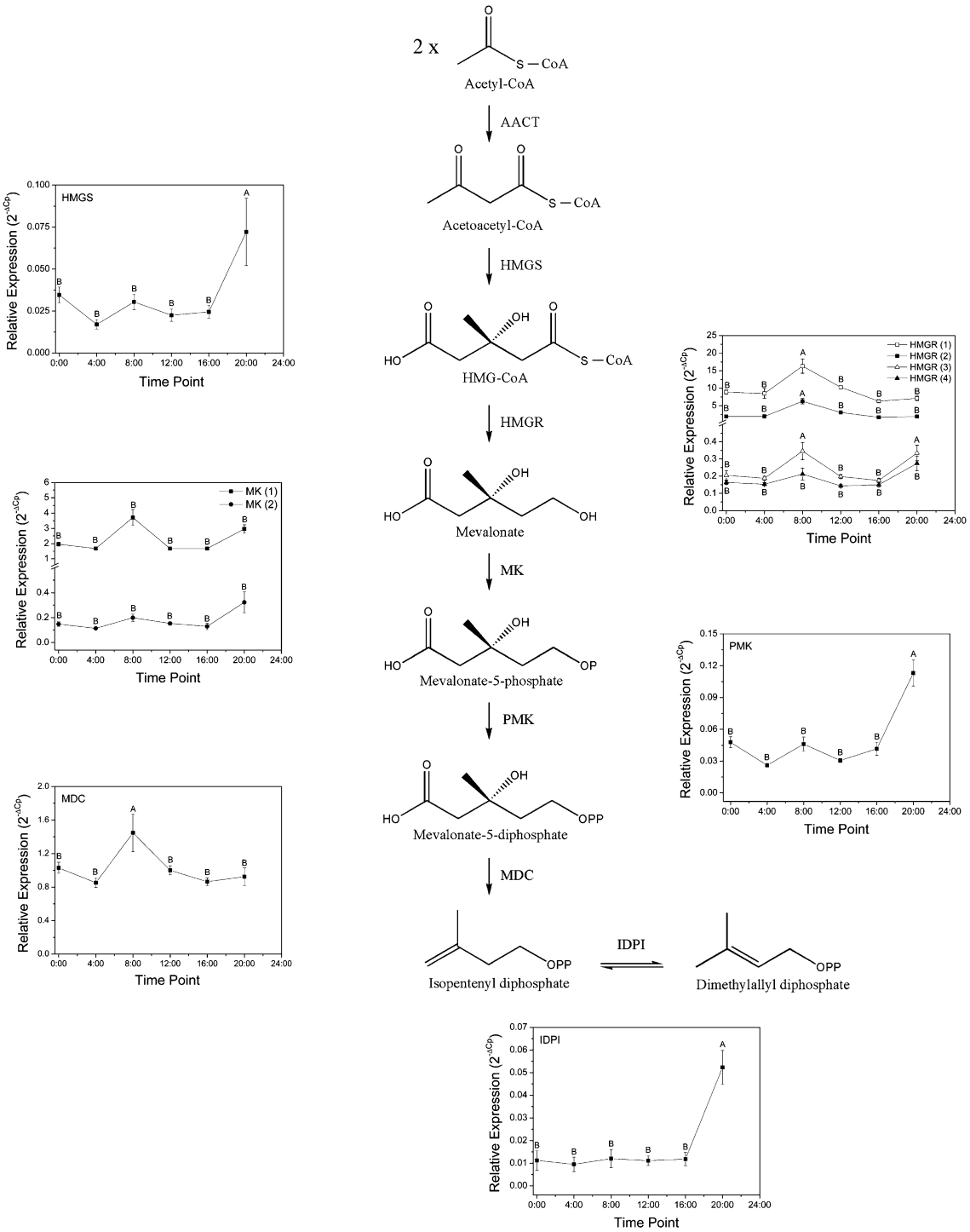

Fig. 8. Relative expression analysis of mevalonate (MVA) pathway genes in *A. chinensis* flowers. All genes were identified from an in-house *Actinidia* expressed sequence tag database collection (Crowhurst *et al.*, 2008). The indicated enzymes are acetyl-CoA/acetyl-CoA C-acetyltransferase (AACT), 3-hydroxy-3-methylglutaryl-CoA synthase (HMGS), 3-hydroxy-3-methylglutaryl-CoA reductase (HMGR), mevalonate kinase (MK), phosphomevalonate kinase (PMK), mevalonate-5-diphosphate decarboxylase (MDC), and isopentenyl diphosphate isomerase (IDPI). Expression levels of the MVA pathway genes were determined using the primers listed in Table S2. Primer efficiencies were between 1.94 and 2.0. *MVA* expression levels were compared to the reference gene *EF1α*, as indicated in Fig. 7. Data are presented as mean ± SEM ($n = 4$). Means labelled without a common letter are significantly different ($P < 0.05$).

Bach, 2000). The accumulation of (*E*,*E*)-farnesol in *A. chinensis* flowers suggests that farnesyl pyrophosphatase activity (Nah *et al.*, 2001) is elevated and/or that the ability to regenerate FDP through the successive phosphorylation of farnesol to farnesyl phosphate and farnesyl phosphate to FDP (Thai *et al.*, 1999; Hemmerlin and Bach, 2000; Hemmerlin *et al.*, 2006; Fitzpatrick *et al.*, 2011) is decreased. However, the later explanation seems less

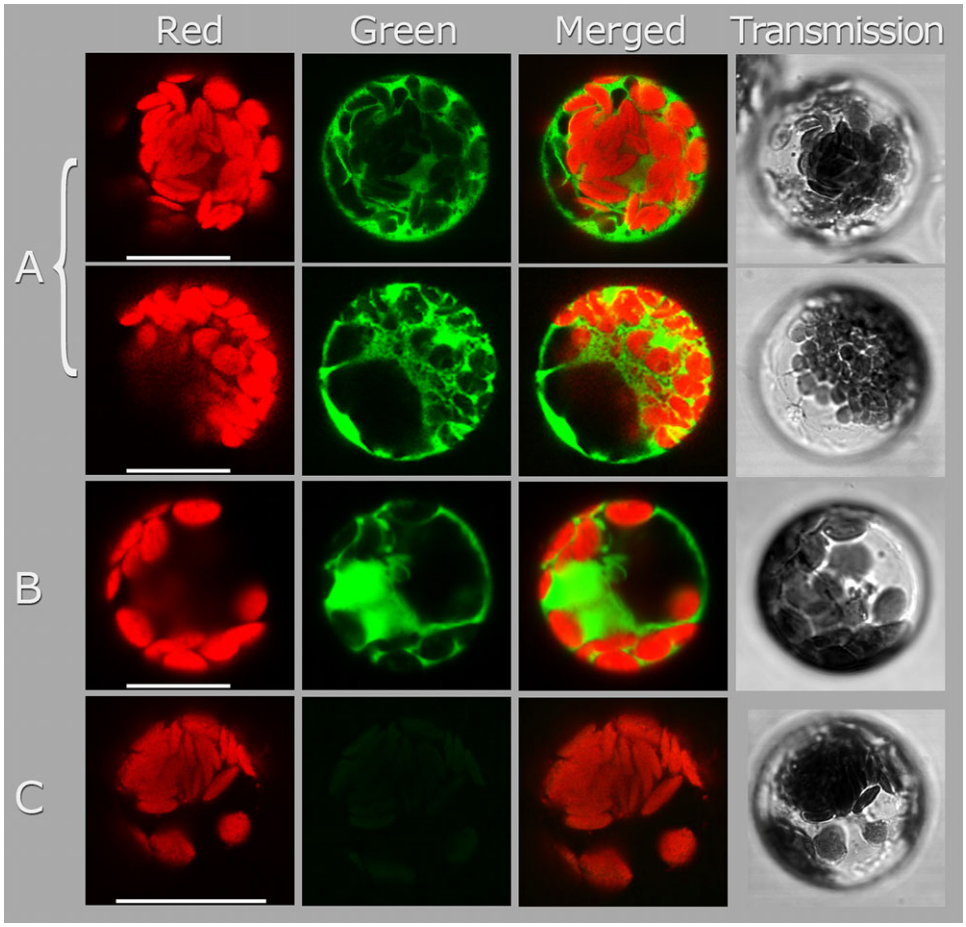

Fig. 9. Subcellular localization of *AcNES1* in *Arabidopsis* leaf protoplasts. The full-length coding region of *AcNES1* was fused to the GFP reporter gene in the vector p326S-GFP to produce the p326-AcNES1/SGFP construct. The fusion construct were then transferred into *Arabidopsis* protoplasts and analysed by confocal laser scanning microscopy for GFP expression. The red columns shows chlorophyll autofluorescence, the green column shown GFP fluorescence, the merged column shows combined chlorophyll autofluorescence and GFP fluorescence, and the transmission column shows light-microscopy images of the intact protoplasts. (A) p326-AcNES1/SGFP, in duplicate from two independent experiments. (B) Control p326-SGFP construct (expressed in the cytosol). (C) No-DNA control. Bars, 25 μm.

plausible given that there is significant turnover of the accumulated farnesol occurring (Fig. 2). The uptake of farnesol by plant cells and incorporation into sterols, proteins, and ubiquinone is likely to account for most of this turnover (Thai *et al.*, 1999; Hemmerlin and Bach, 2000; Hartmann and Bach, 2001), although 7–10% can be accounted for by the conversion of farnesol to farnesal (Supplementary Fig. S3) and up to ~6% is glycosylated (Fig. 3D). Although reasons for the high levels of (*E*,*E*)-farnesol accumulation remain to be determined, it is likely that the consequence of this accumulation will be a depleted pool of FDP available to AcNES1 and hence a diminished capacity for floral sesquiterpene production in *A. chinensis*.

Our work also shows that the regulation of FDP flux in *A. chinensis* flowers and hence sesquiterpene production is likely to be modulated by a number of different MVA pathway genes (Fig. 8). Specifically, the peak levels of *HMGR* RNA expression (Fig. 8) were found to correlate with the day-time accumulation profile of (*E*)-nerolidol and (*E*,*E*)-farnesol (Fig. 2). Moreover, the inverse correlation that exists between the day-time increases in (*E*,*E*)-farnesol accumulation and decreases in *HMGR* expression levels (Figs. 2 and 8 respectively) indicates that high (*E*,*E*)-farnesol concentrations may down-regulate floral *HMGR* expression and/or HMGR enzyme activity. While farnesol treatment has been shown to increase both *HMGR* mRNA and apparent enzyme activity levels in tobacco cells (Hemmerlin and Bach, 2000) it has also been shown to down-regulate HMGR enzyme activity in yeast as a consequence of induced structural changes following farnesol binding (Shearer and Hampton, 2005).

In this study we have identified a sesqui-TPS gene that accounts for (*E*)-nerolidol production in *A. chinensis* flowers. Moreover, we have provided evidence to suggest that elevated (*E*,*E*)-farnesol production in *A. chinensis* flowers reduces their capacity for sesquiterpene biosynthesis. In the future it will be interesting to establish the reasons why such high amounts of the MVA pathway carbon flux ends up as (*E*,*E*)-farnesol and how the enzymes involved in the dephosphorylation of FDP, its salvage from (*E*,*E*)-farnesol, and

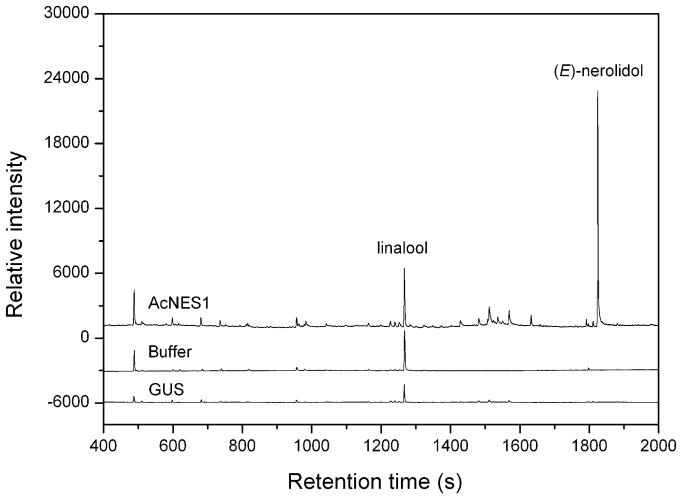

Fig. 10. Transient expression of *AcNES1*. A full-length *AcNES1* cDNA was cloned into the binary vector pHEX2 and transformed into *A. tumefaciens*. Bacterial cell suspensions were infiltrated into the adaxial side of young *N. benthamiana* leaves (in triplicate). Dynamic headspace sampling of volatiles from detached leaves was carried out 14 days after infiltration. Control leaves were infiltrated with buffer-only or with a vector expressing the GUS reporter gene (pHEX2-GUS). Volatiles transiently expressed in *N. benthamiana* are shown after infiltration with *AcNES1* (upper trace), buffer-only (middle trace), and pHEX2-GUS (lower trace).

subsequent reincorporation into primary metabolism are influencing the availability of a precursor crucial for secondary plant metabolic processes.

Supplementary material

Supplementary data are available at *JXB* online.

Supplementary Fig. S1. Rates of monoterpene release from *A. chinensis* flowers during a day/night cycle.

Supplementary Fig. S2. Sequence alignment of AcNES1 with TPS enzymes from fruit and flowers.

Supplementary Fig. S3. (*E*,*E*)-farnesol and (*E*,*E*)-farnesal accumulation in *A. chinensis* flowers.

Supplementary Table S1. Terpene synthase accession numbers.

Supplementary Table S2. Primers.

Acknowledgements

We would like to thank Natalia Dudareva, Dinesh Nagegowda and Jennifer Sturgis for their help in acquiring confocal microscopy data; Inhwan Hwang (POSTEC, Korea) for providing the p326-SGFP vector. We would also like to thank Jinquan Feng for his help with the statistical analysis and Mirco Montefiori, Cyril Brendolise and William Laing for critically reviewing the manuscript. Work at Plant and Food Research was funded by the New Zealand Foundation for Research Science and Technology (CO6X0403).

References

Adam K-P, Zapp J. 1998. Biosynthesis of the isoprene units of chamomile sesquiterpenes. *Phytochemistry* **48,** 953–959.

Aharoni A, Giri AP, Deuerlein S, Griepink F, de Kogel W-J, Verstappen FWA, Verhoeven HA, Jongsma MA, Schwab W, Bouwmeester HJ. 2003. Terpenoid metabolism in wild-type and transgenic *Arabidopsis* plants. *The Plant Cell* **15,** 2866–2884.

Aharoni A, Giri AP, Verstappen FWA, Bertea CM, Sevenier R, Sun Z, Jongsma MA, Schwab W, Bouwmeester HJ. 2004. Gain and loss of fruit flavor compounds produced by wild and cultivated strawberry species. *The Plant Cell* **16,** 3110–3131.

Aharoni A, Jongsma M, Kim T-Y, Ri M-B, Giri A, Verstappen F, Schwab W, Bouwmeester H. 2006. Metabolic engineering of terpenoid biosynthesis in plants. *Phytochemistry Reviews* **5,** 49–58.

Anet EFLJ. 1972. Superficial scald, a functional disorder of stored apples VIII. Volatile products from the autoxidation of alpha-farnesen. *Journal of the Science of Food and Agriculture* **23,** 605–608.

Arigoni D, Eisenreich W, Latzel C, Sagner S, Radykewicz T, Zenk MH, Bacher A. 1999. Dimethylallyl pyrophosphate is not the committed precursor of isopentenyl pyrophosphate during terpenoid biosynthesis from 1-deoxyxylulose in higher plants. *Proceedings of the National Academy of Sciences of the United States of America* **96,** 1309–1314.

Bohlmann J, Meyer-Gauen G, Croteau R. 1998. Plant terpenoid synthases: molecular biology and phylogenetic analysis. *Proceedings of the National Academy of Sciences of the United States of America* **95,** 4126–4133.

Boland W, Gäbler A, Gilbert M, Feng Z. 1998. Biosynthesis of C11 and C16 homoterpenes in higher plants; stereochemistry of the C–C-bond cleavage reaction. *Tetrahedron* **54,** 14725–14736.

Bouwmeester HJ, Verstappen FWA, Posthumus MA, Dicke M. 1999. Spider mite-induced (3*S*)-(*E*)-nerolidol synthase activity in cucumber and Lima bean. The first dedicated step in acyclic C11-homoterpene biosynthesis. *Plant Physiology* **121,** 173–180.

Cane DE. 1990. Enzymic formation of sesquiterpenes. *Chemical Reviews* **90,** 1089–1103.

Chen X, Yauk Y, Nieuwenhuizen NJ, Matich AJ, Wang MY, Perez RL, Atkinson RG, Beuning LL. 2010. Characterisation of an (*S*)-linalool synthase from kiwifruit (*Actinidia arguta*) that catalyses the first committed step in the production of floral lilac compounds. *Functional Plant Biology* **37,** 232–243.

Comeskey DJ, Bunn BJ, Fielder S. 2004. Stereospecific synthesis of all four isomeric 6,8-heneicosadien^{-1}1-ones: sex pheromone components of the painted apple moth *Teia anartoides*. *Tetrahedron Letters* **45,** 7651–7654.

Croteau R. 1987. Biosynthesis and catabolism of monoterpenoids. *Chemical Reviews* **87,** 929–954.

Croteau R, Alonso WR, Koepp AE, Johnson MA. 1994. Biosynthesis of monoterpenes: partial purification, characterization, and mechanism of action of 1,8-cineole synthase. *Archives of Biochemistry and Biophysics* **309,** 184–192.

Crowhurst R, Gleave A, MacRae E, *et al*. 2008. Analysis of expressed sequence tags from *Actinidia*: applications of a cross

species EST database for gene discovery in the areas of flavor, health, color and ripening. *BMC Genomics* **9,** 351.

Danner H, Boeckler GA, Irmisch S, Yuan JS, Chen F, Gershenzon J, Unsicker SB, Köllner TG. 2011. Four terpene synthases produce major compounds of the gypsy moth feeding-induced volatile blend of Populus trichocarpa. *Phytochemistry* **72,** 897–908.

Degenhardt J, Gershenzon J. 2000. Demonstration and characterization of (*E*)-nerolidol synthase from maize: a herbivore-inducible terpene synthase participating in (*3E*)-4,8-dimethyl^{-1},3,7-nonatriene biosynthesis. *Planta* **210,** 815–822.

Dicke M, Baldwin IT. 2010. The evolutionary context for herbivore-induced plant volatiles: beyond the 'cry for help'. *Trends in Plant Science* **15,** 167–175.

Donath J, Boland W. 1995. Biosynthesis of acyclic homoterpenes: enzyme selectivity and absolute configuration of the nerolidol precursor. *Phytochemistry* **39,** 785–790.

Dudareva N, Andersson S, Orlova I, Gatto N, Reichelt M, Rhodes D, Boland W, Gershenzon J. 2005. The nonmevalonate pathway supports both monoterpene and sesquiterpene formation in snapdragon flowers. *Proceedings of the National Academy of Sciences of the United States of America* 933–938.

Dudareva N, Cseke L, Blanc VM, Pichersky E. 1996. Evolution of floral scent in *Clarkia*: novel patterns of *S*-linalool synthase gene expression in the *C. breweri* flower. *The Plant Cell* **8,** 1137–1148.

Dudareva N, Martin D, Kish CM, Kolosova N, Gorenstein N, Faldt J, Miller B, Bohlmann J. 2003. (*E*)-β-ocimene and myrcene synthase genes of floral scent biosynthesis in snapdragon: function and expression of three terpene synthase genes of a new terpene synthase subfamily. *The Plant Cell* **15,** 1227–1241.

Dudareva N, Pichersky E. 2006. Floral scent metabolic pathways: their regulation and evolution. *Biology of Floral Scent* 55–78.

Eisenreich W, Schwarz M, Cartayrade A, Arigoni D, Zenk MH, Bacher A. 1998. The deoxyxylulose phosphate pathway of terpenoid biosynthesis in plants and microorganisms. *Chemistry and Biology* **5,** R221.

Emanuelsson O, Nielsen H, Brunak S, von Heijne G. 2000. Predicting subcellular localization of proteins based on their N-terminal amino acid sequence. *Journal of Molecular Biology* **300,** 1005–1016.

Emanuelsson O, Nielsen H, von Heijne G. 1999. ChloroP, a neural network-based method for predicting chloroplast transit peptides and their cleavage sites. *Protein Science* **8,** 978–984.

Fitzpatrick AH, Bhandari J, Crowell DN. 2011. Farnesol kinase is involved in farnesol metabolism, ABA signaling and flower development in *Arabidopsis*. *The Plant Journal* **66,** 1078–1088.

Gondet L, Weber T, Maillot-Vernier P, Benveniste P, Bach TJ. 1992. Regulatory role of microsomal 3-hydroxy-3-methylglutaryl-coenzyme a reductase in a tobacco mutant that overproduces sterols. *Biochemical and Biophysical Research Communications* **186,** 888–893.

Goodwin TW. 1977. The prenyl lipids of the membranes of higher plants. In: M Tevini, HK Lichtenthaler, eds. *Lipids and Lipid Polymers in Higher Plants*. Berlin: Springer Verlag, pp 29–44.

Green S, Friel EN, Matich A, Beuning LL, Cooney JM, Rowan DD, MacRae E. 2007. Unusual features of a recombinant apple alpha-farnesene synthase. *Phytochemistry* **68,** 176–188.

Greenhagen B, Chappell J. 2001. Molecular scaffolds for chemical wizardry: learning nature's rules for terpene cyclases. *Proceedings of the National Academy of Sciences of the United States of America* **98,** 13479–13481.

Harborne JB. 1991. Recent advances in the ecological chemistry of plant terpenoids. In: JB Harborne, FA Tomas-Barberan, eds, *Ecological Chemistry and Biochemistry of Plant Terpenoids*. Oxford: Clarendon Press, pp 396–426.

Hartmann M-A, Bach TJ. 2001. Incorporation of all-trans-farnesol into sterols and ubiquinone in *Nicotiana tabacum* L. cv Bright Yellow-2 cell cultures. *Tetrahedron Letters* **42,** 655–657.

Hellens R, Allan A, Friel E, Bolitho K, Grafton K, Templeton M, Karunairetnam S, Gleave A, Laing W. 2005. Transient expression vectors for functional genomics, quantification of promoter activity and RNA silencing in plants. *Plant Methods* **1,** 13.

Hemmerlin A, Bach TJ. 2000. Farnesol-induced cell death and stimulation of 3-hydroxy-3-methylglutaryl-coenzyme A reductase activity in tobacco cv Bright Yellow-2 cells. *Plant Physiology* **123,** 1257–1268.

Hemmerlin A, Hoeffler J-F, Meyer O, Tritsch D, Kagan IA, Grosdemange-Billiard C, Rohmer M, Bach TJ. 2003. Cross-talk between the cytosolic mevalonate and the plastidial methylerythritol phosphate pathways in tobacco bright yellow-2 cells. *Journal of Biological Chemistry* **278,** 26666–26676.

Hemmerlin A, Reents R, Mutterer J, Feldtrauer J-F, Waldmann H, Bach TJ. 2006. Monitoring farnesol-induced toxicity in tobacco BY-2 cells with a fluorescent analog. *Archives of Biochemistry and Biophysics* **448,** 93–103.

Hey SJ, Powers SJ, Beale MH, Hawkins ND, Ward JL, Halford NG. 2006. Enhanced seed phytosterol accumulation through expression of a modified HMG-CoA reductase. *Plant Biotechnology Journal* **4,** 219–229.

Keller RK, Thompson R. 1993. Rapid synthesis of isoprenoid diphosphates and their isolation in one step using either thin layer or flash chromatography. *Journal of Chromatography A* **645,** 161–167.

Kreck M, Püschel S, Wüst M, Mosandl A. 2002. Biogenetic studies in *Syringa vulgaris* L.: synthesis and bioconversion of deuterium-labeled precursors into lilac aldehydes and lilac alcohols. *Journal of Agricultural and Food Chemistry* **51,** 463–469.

Lee YJ, Kim DH, Kim Y-W, Hwang I. 2001. Identification of a signal that distinguishes between the chloroplast outer envelope membrane and the endomembrane system *in vivo*. *The Plant Cell* **13,** 2175–2190.

Lesburg CA, Caruthers JM, Paschall CM, Christianson DW. 1998. Managing and manipulating carbocations in biology: terpenoid cyclase structure and mechanism. *Current Opinion in Structural Biology* **8,** 695–703.

Lewinsohn E, Schalechet F, Wilkinson J, *et al*. 2001. Enhanced levels of the aroma and flavor compound *S*-linalool by metabolic engineering of the terpenoid pathway in tomato fruits. *Plant Physiology* **127,** 1256–1265.

Lichtenthaler HK. 1999. The 1-deoxy-D-xylulose-5-phosphate pathway of isoprenoid biosynthesis in plants. *Annual Review of Plant Physiology and Plant Molecular Biology* **50,** 47–65.

Lichtenthaler HK, Rohmer M, Schwender J. 1997. Two independent biochemical pathways for isopentenyl diphosphate and isoprenoid biosynthesis in higher plants. *Physiologia Plantarum* **101,** 643.

Martin D, Aubourg S, Schouwey M, Daviet L, Schalk M, Toub O, Lund S, Bohlmann J. 2010. Functional annotation, genome organization and phylogeny of the grapevine (*Vitis vinifera*) terpene synthase gene family based on genome assembly, FLcDNA cloning, and enzyme assays. *BMC Plant Biology* **10,** 226.

Matich AJ, Bunn BJ, Hunt MB. 2010. The enantiomeric composition of linalool and linalool oxide in the flowers of kiwifruit (*Actinidia*) species. *Chirality* **22,** 110–119.

Matich AJ, Young H, Allen JM, Wang MY, Fielder S, McNeilage MA, MacRae EA. 2003. *Actinidia arguta*: volatile compounds in fruit and flowers. *Phytochemistry* **63,** 285–301.

Maurey K, Wolf F, Golbeck J. 1986. 3-Hydroxy-3-methylglutaryl coenzyme A reductase activity in *Ochromonas malhamensis*: a system to study the relationship between enzyme activity and rate of steroid biosynthesis. *Plant Physiology* **82,** 523–527.

Mondello L, Dugo P, Dugo G. 2002. The chiral compounds of citrus essential oils. In: G Dugo, A Di Giacomo, eds, *Citrus The Genus Citrus*. London: Taylor and Francis, pp 461–495.

Montefiori M, Espley RV, Stevenson D, Cooney J, Datson PM, Saiz A, Atkinson RG, Hellens RP, Allan AC. 2011. Identification and characterisation of F3GT1 and F3GGT1, two glycosyltransferases responsible for anthocyanin biosynthesis in red-fleshed kiwifruit (*Actinidia chinensis*). *The Plant Journal* **65,** 106–118.

Muñoz-Bertomeu J, Sales E, Ros R, Arrillaga I, Segura J. 2007. Up-regulation of an N-terminal truncated 3-hydroxy-3-methylglutaryl CoA reductase enhances production of essential oils and sterols in transgenic *Lavandula latifolia*. *Plant Biotechnology Journal* **5,** 746–758.

Nagegowda D, Gutensohn M, Wilkerson C, Dudareva N. 2008. Two nearly identical terpene synthases catalyze the formation of nerolidol and linalool in snapdragon flowers. *The Plant Journal* **55,** 224–239.

Nah J, Song S-J, Back K. 2001. Partial characterization of farnesyl and geranylgeranyl diphosphatases induced in rice seedlings by UV-C irradiation. *Plant and Cell Physiology* **42,** 864–867.

Nes WR, McKean ML. 1977. Occurence, physiology and ecology of sterols. In: WR Nes, ML McKean, eds, *Biochemistry of Steroids and Other Isopentenoids*. Baltimore: University Park Press, pp 411–533.

Nieuwenhuizen NJ, Beuning LL, Sutherland PW, Sharma NN, Cooney JM, Bieleski LRF, Shroeder R, MacRae EA, Atkinson RG. 2007. Identification and characterisation of acidic and novel basic forms of actinidin, the highly abundant cysteine protease from kiwifruit. *Functional Plant Biology* **34,** 946–961.

Nieuwenhuizen NJ, Wang MY, Matich AJ, Green SA, Chen X, Yauk Y-K, Beuning LL, Nagegowda DA, Dudareva N, Atkinson RG. 2009. Two terpene synthases are responsible for the major sesquiterpenes emitted from the flowers of kiwifruit (*Actinidia deliciosa*). *Journal of Experimental Botany* **60,** 3203–3219.

Pichersky E, Gershenzon J. 2002. The formation and function of plant volatiles: perfumes for pollinator attraction and defense. *Current Opinion in Plant Biology* **5,** 237–243.

Rice P, Longden I, Bleasby A. 2000. EMBOSS: the European Molecular Biology Open Software Suite. *Trends in Genetics* **16,** 276–277.

Rodriguez-Concepcion M, Boronat A. 2002. Elucidation of the methylerythritol phosphate pathway for isoprenoid biosynthesis in bacteria and plastids. A metabolic milestone achieved through genomics. *Plant Physiology* **130,** 1079–1089.

Rohmer M. 1999. The discovery of a mevalonate-independent pathway for isoprenoid biosynthesis in bacteria, algae and higher plants. *Natural Product Reports* **16,** 565.

Saitou N, Nei M. 1987. The neighbor-joining method: a new method for reconstructing phylogenetic trees. *Molecular Biology and Evolution* **4,** 406–425.

Savage T, Hatch M, Croteau R. 1994. Monoterpene synthases of *Pinus contorta* and related conifers. A new class of terpenoid cyclase. *Journal of Biological Chemistry* **269,** 4012–4020.

Schnee C, Kollner TG, Gershenzon J, Degenhardt J. 2002. The maize gene *terpene synthase 1* encodes a sesquiterpene synthase catalyzing the formation of (*E*)-β-farnesene, (*E*)-nerolidol, and (*E*,*E*)-farnesol after herbivore damage. *Plant Physiology* **130,** 2049–2060.

Shearer AG, Hampton RY. 2005. Lipid-mediated, reversible misfolding of a sterol-sensing domain protein. *The EMBO Journal* **24,** 149–159.

Spurgeon SL, Porter JW. 1981. Introductions. In: JW Porter, S Spurgeon, eds, *Biosynthesis of Isoprenoid Compounds,* limited edn. New York: John Wiley and Sons, pp 1–46.

Studier FW. 2005. Protein production by auto-induction in high density shaking cultures. *Protein Expression and Purification* **41,** 207–234.

Tamura K, Dudley J, Nei M, Kumar S. 2007. MEGA4: Molecular Evolutionary Genetics Analysis (MEGA) software version 4.0. *Molecular Biology and Evolution* **24,** 1596–1599.

Thai L, Rush JS, Maul JE, Devarenne T, Rodgers DL, Chappell J, Waechter CJ. 1999. Farnesol is utilized for isoprenoid biosynthesis in plant cells via farnesyl pyrophosphate formed by successive monophosphorylation reactions. *Proceedings of the National Academy of Sciences of the United States of America* **96,** 13080–13085.

Tholl D, Chen F, Petri J, Gershenzon J, Pichersky E. 2005. Two sesquiterpene synthases are responsible for the complex mixture of sesquiterpenes emitted from *Arabidopsis* flowers. *The Plant Journal* **42,** 757–771.

Thompson JD, Gibson TJ, Plewniak F, Jeanmougin F, Higgins DG. 1997. The CLUSTAL_X windows interface: flexible strategies for multiple sequence alignment aided by quality analysis tools. *Nucleic Acids Research* **25,** 4876–4882.

Unsicker SB, Kunert G, Gershenzon J. 2009. Protective perfumes: the role of vegetative volatiles in plant defense against herbivores. *Current Opinion in Plant Biology* **12,** 479–485.

Wu S, Schalk M, Clark A, Miles RB, Coates R, Chappell J. 2006. Redirection of cytosolic or plastidic isoprenoid precursors elevates terpene production in plants. *Nature Biotechnology* **24,** 1441–1447.

Young H, Paterson VJ. 1995. Characterisation of bound flavour components in kiwifruit. *Journal of the Science of Food and Agriculture* **68,** 257–260.

Zuckerkandl E, Pauling L. 1965. Evolutionary divergence and convergence in proteins. In: V Bryson, HJ Vogel, eds, *Evolving Genes and Proteins*. New York: Academic Press, pp 97–166.